

Selecting ultra-faint dwarf candidate progenitors in cosmological N-body simulations at high redshifts

Mohammadtaher Safarzadeh¹^{*}, Alexander P. Ji^{2,†}, Gregory A. Dooley³, Anna Frebel³, Evan Scannapieco¹, Facundo A. Gómez^{4,5}, Brian W. O’Shea^{6,7,8,9}

¹*School of Earth and Space Exploration, Arizona State University, Tempe, AZ 85287-1404, USA*

²*The Observatories of the Carnegie Institution of Washington, 813 Santa Barbara St., Pasadena, CA 91101, USA*

[†]*Hubble Fellow*

³*Department of Physics, Kavli Institute for Astrophysics and Space Research, Massachusetts Institute of Technology, 77 Massachusetts Avenue, Cambridge, MA 02139, USA*

⁴*Instituto de Investigación Multidisciplinar en Ciencia y Tecnología, Universidad de La Serena, Raúl Bitrán 1305, La Serena, Chile*

⁵*Departamento de Física y Astronomía, Universidad de La Serena, Av. Juan Cisternas 1200 N, La Serena, Chile*

⁶*Department of Computational Mathematics, Science and Engineering, Michigan State University, MI, 48823, USA*

⁷*Department of Physics and Astronomy, Michigan State University, MI, 48823, USA*

⁸*National Superconducting Cyclotron Laboratory, Michigan State University, MI, 48823, USA*

⁹*Joint Institute for Nuclear Astrophysics - Center for the Evolution of the Elements, USA*

13 December 2017

ABSTRACT

The smallest satellites of the Milky Way ceased forming stars during the epoch of reionization and thus provide archaeological access to galaxy formation at $z > 6$. Numerical studies of these ultra-faint dwarf galaxies (UFDs) require expensive cosmological simulations with high mass resolution that are carried out down to $z = 0$. However, if we are able to statistically identify UFD host progenitors at high redshifts *with relatively high probabilities*, we can avoid this high computational cost. To find such candidates, we analyze the merger trees of Milky Way type halos from the high-resolution *Caterpillar* suite of dark matter only simulations. Satellite UFD hosts at $z = 0$ are identified based on four different abundance matching techniques. All the halos at high redshifts are traced forward in time in order to compute the probability of surviving as satellite UFDs today. Our results show that selecting potential UFD progenitors based solely on their mass at $z=12$ (8) results in a 10% (20%) chance of obtaining a surviving UFD at $z = 0$. We find that the progenitors of surviving satellite UFDs have lower virial ratios (η), and are preferentially located at large distances from the main MW progenitor, while they show no correlation with concentration parameter. Halos with favorable locations and virial ratios are ≈ 3 times more likely to survive as satellite UFD candidates at $z = 0$.

Key words: Galaxies: Dwarf; Galaxies: Local Group ; Galaxies: statistics

1 INTRODUCTION

The faintest satellite galaxies of the Milky Way (MW) preserve an archaeological snapshot of galaxy formation and chemical enrichment in the early universe. These ultra-faint dwarf galaxies (UFDs) have luminosities of only $L \approx 10^{2.5-5} L_{\odot}$ (e.g. [McConnachie 2012](#)), but their stars display large velocity dispersions implying they reside in dark matter halos of mass $\sim 10^7 - 10^9 M_{\odot}$ ([Simon & Geha 2007](#); [Strigari et al. 2008](#); [Simon et al. 2011](#)). The stellar populations

of UFDs are all very old (> 12 Gyr [Brown et al. 2014](#); [Weisz et al. 2014](#)) and metal-poor ($[Fe/H] < -2$, e.g. [Kirby et al. 2008](#); [Frebel & Bromm 2012](#); [Vargas et al. 2013](#)), implying that UFDs formed nearly all of their stars prior to reionization (e.g. [Bullock et al. 2000](#); [Bovill & Ricotti 2009, 2011](#)). Observations of the population of UFDs are not complete ([Tollerud et al. 2008](#); [Hargis et al. 2014](#)), and are still being discovered in the Milky Way ([Drlica-Wagner et al. 2015](#); [Koposov et al. 2015](#)) and other nearby galaxies ([Lee et al. 2017](#)).

The star formation history of UFDs and their host halo characteristics and accretion history have been stud-

* E-mail: mts@asu.edu

ied through various techniques (Gnedin & Kravtsov 2006; Salvadori & Ferrara 2009; Bovill & Ricotti 2011; Garrison-Kimmel et al. 2014; Wheeler et al. 2015b; Bland-Hawthorn et al. 2015; Garrison-Kimmel et al. 2017a; Sawala et al. 2017; Jeon et al. 2017). However, direct cosmological hydrodynamic simulations to study UFDs remain challenging. Simulation boxes with comoving sizes of ≈ 10 Mpc/h on a side (Boylan-Kolchin et al. 2016) would be required in order to self-consistently simulate the MW in its environment and also to capture the reionization’s impact on the star formation history of galaxies due to the patchiness of the process. With such box sizes, a full radiative-hydro simulation with a dark matter particle mass of $\leq 10^4 M_\odot$ needed to resolve UFD host halos requires approximately 10 Million core-hours to simulate down to redshifts $z \approx 8 - 10$ (Xu et al. 2016). Therefore, it is currently impossible to simulate such boxes down to $z = 0$ to identify the survived halos with star formation histories resembling UFDs around the Milky Way (though isolated UFDs can still be studied; e.g. Wheeler et al. 2015a; Jeon et al. 2017). In this situation, it is useful to have a method to predict the fate of the halos given what we know about their properties at high redshifts.

The fate of halos given their mass has been studied in the literature in the context of classical dSph galaxies when the satellite to host halo mass ratio is $m_{\text{sat}}/M_{\text{host}} > 10^{-3}$. Sales et al. (2007) studied the characteristics of the halos that merge into the main host and those that survive in a MW type halo and find that mass and eccentricity of the orbit of the satellite determines the fate of a satellite through dynamical friction (Boylan-Kolchin et al. 2008). They find that satellites that merge into the host tend to have more eccentric orbits compared to those that survive. Moreover, the merging satellites tend to be accreted into the main host at earlier times, meaning they spend more time within the virial radius of the host and experience dynamical friction on a longer timespan. Likewise, Klimentowski et al. (2010) find the survival probability depends on the number of times a satellites experiences a pericenter passage.

In this paper, we focus on statistics of the surviving halos given their mass and other characteristics that tie them to the UFDs. We analyze the merger trees of MW analogs constructed based on N-body simulations to study the characteristics of the halos at high redshifts ($z > 4$) that survive as UFD host halos today, corresponding to a satellite-to-halo mass ratio of $\sim 10^{-5}$. Such study would require a particle mass of $\approx 10^4 M_\odot$ to at least resolve halos of mass $M \approx 10^7 M_\odot$ with 1000 dark matter particles. The *Caterpillar* simulation suite (Griffen et al. 2016a,b) is a set of zoom-in N-body simulations on 32 MW-type halos that provides us the tools for such study. We identify UFDs at $z = 0$ based on various abundance matching (AM) techniques that we describe in the methods section. We first focus on the halo mass as the primary informant of survivability of the halos as UFD hosts today. We study what fraction of the halos at a given mass and redshift bin (a) survive as UFD hosts, (b) merge into the main host, (c) merge into a classical dSph galaxy, and (d) merge into a UFD candidate halo. We then consider other dynamical parameters such as distance from the main progenitor, virial ratio ($\eta \equiv 2T/|U|$) where T and U are the total kinetic and potential of a halo, and concentration parameter of the halos to explore if these parameters drive the survivability of the halos as UFD hosts today.

In §2 we describe our method in more detail. In §3 we present our results, and in §4 we discuss our results and give conclusions.

2 METHOD

2.1 Simulations

We use 32 N-body zoom-in simulations of Milky Way analogs from the *Caterpillar* simulation suite (Griffen et al. 2016a,b). These host halos were selected from a $100 h^{-1}$ Mpc³ box to have masses and formation histories consistent with that of the Milky Way ($0.7 \times 10^{12} M_\odot \leq M_{\text{vir}} \leq 3 \times 10^{12} M_\odot$) and were re-simulated to $z = 0$ with particle mass $m_p = \approx 3 \times 10^4 M_\odot$, and comoving softening length of 113 pc. Initial conditions were generated from MUSIC (Hahn & Abel 2011) for a Planck 2013 cosmology ($\Omega_m = 0.32$, $\Omega_\Lambda = 0.68$, $n_s = 0.96$, $\sigma_8 = 0.83$, $h = 0.6711$ Planck Collaboration et al. 2014). The simulations were run with GADGET-3 and GADGET-4 (Springel 2005). The ROCKSTAR halo finder (Behroozi et al. 2013a with iterative unbinding implemented as described in Griffen et al. 2016b) was used and the associated merger trees was constructed with CONSISTENT-TREES (Behroozi et al. 2013c). In this paper, our analysis is conducted entirely on these merger trees. For more details, see Griffen et al. (2016b).

Virial halo masses are defined by the Bryan & Norman (1998) definition. We refer to the main Milky Way halo ($M_{\text{vir}} \approx 10^{12} M_\odot$) in each simulation as the “host halo.” Most of the 32 zoom-in simulations have volumes uncontaminated by low-resolution particles out to 1 Mpc at $z = 0$, but throughout this paper we only consider halos that end up within the Milky Way’s virial radius at $z = 0$. All “peak” quantities are defined as occurring at the snapshot where a halo’s main branch reaches its maximum mass; i.e. M_{peak} is the maximum mass of a halo over its main branch, and v_{peak} is v_{max} at that time. The virial ratio is defined as $\eta = 2T/|U|$, where T and $|U|$ are kinetic and gravitational energies of the halos and the ratio $T/|U|$ is computed by ROCKSTAR. We also consider halo concentrations, but these tend to be poorly defined for subhalos. Therefore, to estimate the concentration parameter, we adopt the following formula which is a more robust estimate than r_{vir}/r_s (Springel et al. 2008; Dooley et al. 2014) which we denote as c_{vmax} :

$$\frac{c^3}{\ln(1+c) - c/(1+c)} = 0.216 \left(\frac{V_{\text{max}}}{H_0 r_{\text{vmax}}} \right)^2 \quad (1)$$

2.2 Selecting UFDs and their progenitors

To trace UFD progenitors, we must first identify a population of dark matter halos at $z = 0$ as UFD host candidates. Ideally this would be done by constructing a physical model that predicts the luminosities of all subhalos. However, the relevant physics for forming low-luminosity galaxies is still not completely certain (e.g., Lu et al. 2017), and it is still challenging to directly simulate a Milky Way galaxy while resolving its satellites (Fattahi et al. 2016).

Various methods have been adopted to identify UDF candidates from high resolution N-Body simulations based on abundance matching (AM) techniques (Moster et al. 2013; Behroozi et al. 2013d; Garrison-Kimmel et al. 2014,

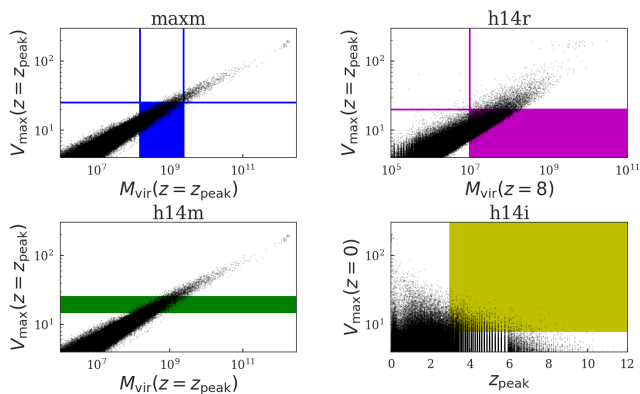


Figure 1. Selection criteria for UFDs. Each panel shows all halos at $z = 0$ in the main host (black points), as well as the selection cuts defined to select UFDs (colored lines and shaded region; the same colors are used for later plots). Model h14i also has $v_{\text{peak}} < 25 \text{ km s}^{-1}$ applied.

2017a; Brook et al. 2014; Jethwa et al. 2016). Given the method of choice, the statistics of the UFD candidates such as their number density and spatial distribution can also vary (Garrison-Kimmel et al. 2014; Hargis et al. 2014; Dooley et al. 2016a). Here, we choose four simple definitions based on a halo’s mass and accretion history, which are shown in Figure 1 and described as follows:

- **maxm:** Surviving $z = 0$ halos with stellar mass between $10^3 - 2 \times 10^5 M_{\odot}$ using the abundance matching relation of Garrison-Kimmel et al. (2014):

$$M_{\star}(M_{\text{peak}}) = 3 \times 10^6 M_{\odot} \left(\frac{M_{\text{peak}}}{10^{10} M_{\odot}} \right)^{1.92} \quad (2)$$

The luminosity range corresponds to $10^{8.2} M_{\odot} \lesssim M_{\text{peak}} \lesssim 10^{9.4} M_{\odot}$.

- **h14m:** Massive in the past : Surviving $z = 0$ halos with $v_{\text{peak}} > 15 \text{ km s}^{-1}$ (Hargis et al. 2014). These halos are *not* required to have formed prior to reionization.
- **h14r:** Formed before reionization: Surviving $z = 0$ halos with $v_{\text{peak}} < 20 \text{ km s}^{-1}$ and $M_{z=8} > 10^7 M_{\odot}$ (Hargis et al. 2014). These are the halos that are formed before reionization and correspond to the fossil definition of UFDs (Bovill & Ricotti 2011).
- **h14i:** Earliest infall: Surviving $z = 0$ halos with $v_{\text{max},z=0} > 8 \text{ km s}^{-1}$ and $z_{\text{peak}} > 3$ (Hargis et al. 2014). This corresponds to associating UFDs with massive halos that lost most of their gas and dark matter content through stripping processes after they infall into the MW host at $z > 3$ (Kravtsov et al. 2004).

In all UFD selection methods, we only consider objects with $v_{\text{peak}} \leq 25 \text{ km s}^{-1}$. The value of 25 km s^{-1} is consistent with the criterion of circular velocity of the halos being less than $v_c < 20 \text{ km s}^{-1}$ (Bovill & Ricotti 2009) to define pre-reionization fossils based on the combined effect of feedback and cooling in such low mass halos at redshifts of reionization. We also note that all halos that we have defined as UFD candidates are true fossils in that they never reached a mass scale in their entire history beyond the filtering mass corresponding to $v_{\text{fit}} = 20 - 30 \text{ km s}^{-1}$ to be able to accrete

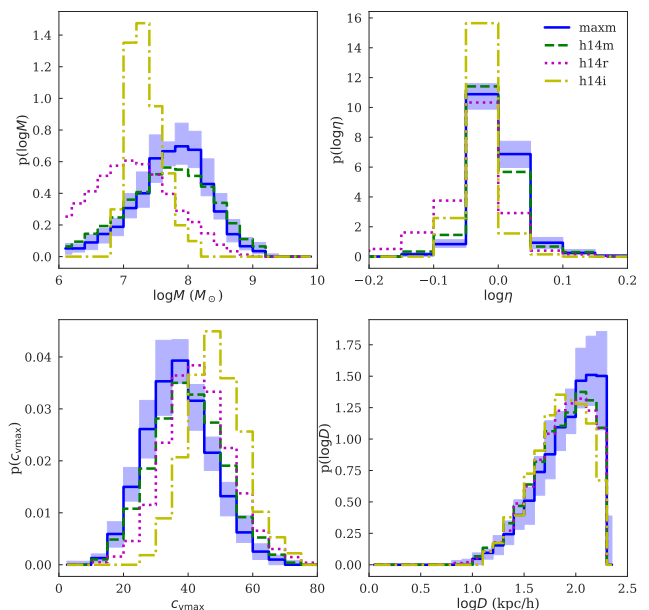


Figure 2. The distribution of the UFD host halos that are selected at $z = 0$ based on the above four AM techniques in mass, virial ratio, concentration parameter, and distance from the main progenitor. The histograms are normalized to better illustrate the differences between the models. The most important differentiator between the models is the mass distribution of the UFD host halo candidates.

gas from the IGM and therefore reignite their star formation and be considered as a polluted system (Gnedin & Kravtsov 2006; Bovill & Ricotti 2011).

The main branch of a $z = 0$ halo is defined by tracing the most massive progenitor at each snapshot. For each MW simulation, we trace the main branch of all halos at $z = 0$ back to a higher redshift z . This halo at redshift z is called the *main progenitor* of the $z = 0$ halo. We only consider objects with mass $> 10^{6.5} M_{\odot}$ at all redshifts. We ignore halos that do not end up within the virial radius of the $z = 0$ host for two reasons. First, the Caterpillar halos are only guaranteed to be uncontaminated by low-mass-resolution particles within the virial radius. Second, nearly all galaxies in the UFD mass range are observed within the Milky Way’s virial radius. Some UFDs are recently discovered outside the local group (LG) (Lee et al. 2017) which shows these systems are ubiquitous though challenging to detect because of their low surface brightness (see also Wheeler et al. 2015a; Dooley et al. 2016b).

The distribution of the UFD candidates that are selected at $z = 0$ based on the above four AM techniques for different dynamical parameters is shown in Figure 2. The histograms are normalized to better reflect the distributions. The largest difference between the models is reflected in the mass distribution of the UFD halo candidates at $z = 0$. The distributions in concentration and radial distance from the center of the halo is about the same for all four models. In all cases the results of the h14i model is more distinct than those of the other models as halos in this model have been processed more efficiently through tidal stripping.

3 RESULTS

3.1 Distribution of halos in various dynamical parameters

The first question we address is: For surviving UFDs today, what is their distribution in various parameters that describe the halo’s dynamical status at high redshifts? We study mass, concentration parameter, virial ratio and the distance from the main progenitor.

We first show the overall distributions of the halos at $z = 8$ for these parameters and compare them to the progenitors of the UFD candidates. The top row of Figure 3 shows the number of all MW and MW’s satellites progenitor halos at $z = 8$ for all the 32 *Caterpillar* halos as a solid black histogram. The dashed lines show all those that survive until $z = 0$. The other colored histograms show, for each parameter, the distribution of those that survive as a satellite UFD candidate (based on four different methods to identify them) at $z = 0$. The bottom row of Figure 3 shows the ratio of the colored and dashed histograms in the top panel to the solid black one. Therefore, the bottom panel of Figure 3 shows the conditional probability that a halo at $z = 8$ survives *intact* as a UFD (colored lines) or ends up as any surviving subhalo (black dashed line) given its mass, virial ratio, concentration parameter, and distance from the main progenitor. In all panels, the shaded regions represent the 68% scatter between the 32 MW host halos in *Caterpillar* (this is effectively the same as dropping the highest and lowest value in each bin).

When showing the distribution in mass, we set a lower limit to $\log(M/M_\odot) \approx 6.5$ because that corresponds to a halo with at least 100 DM particles. We note that by performing hydrodynamical simulations coupled with radiative cooling on individual halos, Bland-Hawthorn et al. (2015) arrive at a physical lower mass limit for a UFD progenitor of $\approx 10^7 M_\odot$. This mass limit is for a halo to survive a SN explosion in the presence of radiative cooling without being modeled in a cosmological setting that could potentially change the results.

Figure 3 shows that halos have the highest probability to survive as UFD defined in the **h14r** model compared to other three models to identify UFD candidates at $z = 0$. The reason being simply that there are more halos at $z = 0$ that satisfy the **h14r** model definition of a UFD host candidate. The lowest probability is associated with the **h14i** model. This is also shown in Hargis et al. (2014). The reason behind this is that in the **h14i** model, we are focusing on those halos that have entered their host halo at $z > 3$ and therefore have had a longer time of experiencing the tidal forces in the host leading to their destruction. However, we note that for the **h14i** case the criterion is a limit on the maximum circular velocity at $z = 0$ as opposed to the other three models where the cut on v_{\max} is imposed at z_{peak} . Though we have imposed a limit for a halo to be identified with at least 100 DM particles at high redshifts, the limit at $z = 0$ is only 10 particles which is the default of the halo finder algorithm. Imposing a 100 DM particle at $z = 0$ similar to high redshift, would reduce the number of candidates at $z = 0$ for the other three models and bring the four models into better agreement with each other.

The population of all the surviving halos (regardless of whether they end up as a UFD candidate or not) and

those that survive as UFDs have similar distribution in distance from the host, concentration, and virial ratio, while they are noticeably different in mass. The survival probability for halos has a flat distribution in mass when we only care about whether they survive as a MW satellite or not. The chances of survival as a UFD candidate peaks around $\log(M/M_\odot) \approx 7.5-8$ at $z = 8$. Therefore, mass is the desirable parameter if we are about to select halos at $z = 8$ to have a higher chance to become UFD candidates as opposed to merging into or surviving as a classical dSph galaxies. Note that we selected UFDs primarily by their halo mass, so essentially there is a high correlation between $M(z = 8)$ and M_{peak} . Indeed around $\log(M/M_\odot) \approx 7.5 - 8.5$ almost all the survived halos are those that survive as a UFD candidate as the difference between the dashed line and the colored lines is shrunk to zero around that mass range (see bottom panel of Figure 3, the distribution in mass). The means by which the knowledge of other parameters describing a halo at high redshifts would inform us about the survival probability is explored in Section 3.3.

It should be noted that between different AM techniques to identify the UFDs at $z = 0$, the **maxm** method, which is an observationally oriented technique, leads to a distribution that is in better agreement with the predictions of **h14m** (massive in the past) model. In other words, comparing colored lines in the bottom panel of Figure 3, the **h14m** line is closer to **maxm** line in all the parameters studied. This could also be read from Figure 1 where one sees that the selection criteria for the **maxm** and **h14m** bracket almost the same parameter space.

3.2 Fate of a halo given its mass

We now turn the question around and ask what is the fate of halos at high redshifts given their mass and specifically what is the probability of surviving as a UFD candidate? We trace all the halos in the simulation box at $z = 8$ (shown as the dashed black histogram in the top panel of Figure 3) down to $z = 0$ and study their fate at $z = 0$ given their mass at $z = 8$. We define five different $z = 0$ categories, tracking halos that:

- Merge into their hosts.
- Merge into classical dSph galaxies, defined as halos with $M_\star > 2 \times 10^5 M_\odot$, or $M_{\text{peak}} > 2.5 \times 10^9 M_\odot$, according to the Garrison-Kimmel et al. (2014) abundance matching model.
- Become the main progenitors of classical dSph galaxies.
- Merge into UFD candidates.
- Become the main progenitors of UFD candidates.

Halos merging into objects with mass range less than UFDs or equal to UFDs but not satisfying the UFD conditions are not studied.

Figure 4 shows the fate of halos at $z = 8$ as a function of their mass for those five categories. In Panel (a) we show the fraction of halos that would merge into the main host and classical dSph galaxies as a function of their mass. The larger probability to merge into the main host for more massive halos is due to the dynamical friction (Chandrasekhar 1943), which is more effective for more massive satellites. Nearly 40% of halos with $M_h \sim 10^7 M_\odot$ merge into the main host, and the probability rises to unity for halos with mass $M_h > 10^9 M_\odot$. Panel (b) shows the probability of becoming

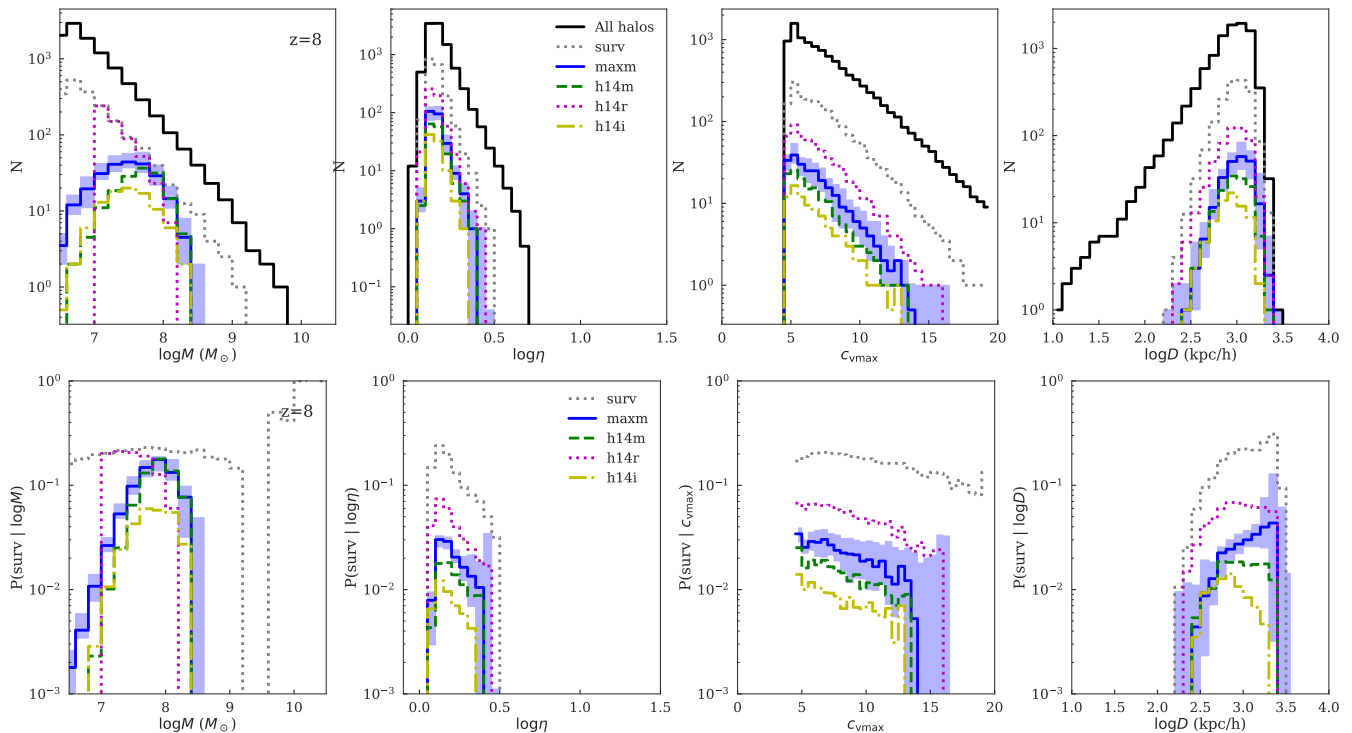


Figure 3. Top: Histogram of halo masses at $z = 8$ in all 32 Caterpillar simulations. Solid black line shows the histogram for all the halos at $z = 8$. Dashed black line shows those halos that survive intact till $z = 0$. Colored lines indicate objects at $z = 8$ that become identified as UFDs according to four different definitions (see text). Bottom: Fraction of halos at $z = 8$ that would survive (dashed line) or be considered as UFDs (colored lines) by $z = 0$. These lines are the results of dividing the colored and dashed lines in the top panel by the solid black line. The shaded regions correspond to 68% MW-to-MW halo scatter.

the main progenitor of a classical dSph galaxy (thick red line) and a UFD candidate based on our four different AM techniques to identify them at $z = 0$. A similar result has been shown in [Bovill & Ricotti \(2011\)](#) where fossils formed in biased regions will merge into non-fossil halos with circular velocities $v_c > 20\text{--}30 \text{ km s}^{-1}$. This result is also consistent with [Gnedin & Kravtsov \(2006\)](#) where they find 5-15% of dwarf satellite galaxies at $z \approx 8$ survive until the present without significant evolution since then. Halos with mass between $\log(M/M_\odot) \approx 7\text{--}8$ have about 10-20% chance of surviving as a UFD based on three of the four different selection cuts (h14m, h14r, and maxm). The yellow line (h14i model) that corresponds to the earliest infall model ([Kravtsov et al. 2004](#)) shows different results compared to the other three AM methods. h14i model only include systems that are accreted into the main host at $z > 3$ and therefore they experience tidal stripping for a rather long time compared with the other three models. Panel (c) shows the probability that a halo merges into a UFD candidate at $z = 0$, which naturally peaks at lower masses compared to what is shown in panel (b). The shaded regions are 68 percentile computed from all the 32 MW halos modeled in *Caterpillar* simulation.

We apply the same procedure at other redshifts (at $z = 4, 6, 8, 10, 12$). In panel (a) of Figure 5 we show the probability of merging into the main host as a function of redshift for a given mass bin. For a halo at given mass, being at higher redshifts increases its probability of merging into the main host. This is intuitive as a halo at higher redshift will grow in mass from $z \approx 12$ to $z \approx 4$ and therefore a smaller halo

at $z \approx 12$ (for example with mass $\approx 10^8 M_\odot$) would have a similar fate as a more massive halo ($10^9 M_\odot$) at $z \approx 8$. The upturn at low masses which is pronounced in the $z = 4$ curve, is a numerical artifact. The halo finder has a difficult time recovering sub halos with large mass ratios between the sub halo and the host, specifically at small distances from the host. This is illustrated in [Behroozi et al. \(2013b\)](#) (See their Figure 10) for a massive host halo in which satellites with small satellite mass ratio are not recovered at small distances from the host. Low mass halos at high redshifts (for example at $z = 12$) merge into a smaller host and the halo finder does not face as much difficulty in correctly tracing them in time.

However, at redshifts $z \approx 4$, the same low mass halos tend to merge into more massive hosts and therefore having smaller satellite-to-host mass ratios. Due to this fact, the merging of these small halos is artificially boosted to higher values contrary to what one would expect from the dynamical friction arguments. Panel (b) shows the redshift evolution of the halos merging into a classical dSph galaxy, which shifts towards larger masses at lower redshifts. Panel (c) shows that the probability of a halo to survive as a UFD shifts towards larger masses at lower redshifts. We have selected “maxm” model as our fiducial case. For example, a halo with mass $\approx 10^{8.5} M_\odot$ has zero chance to survive as a UFD candidate at $z = 12$ while halos of the same mass at $z = 4$ have 40% chance of surviving as a UFD candidate. Panel (d) shows the probability to merge into a UFD candidate as a function of redshift which drops at higher masses at all redshifts. The probability drops to zero at the mass

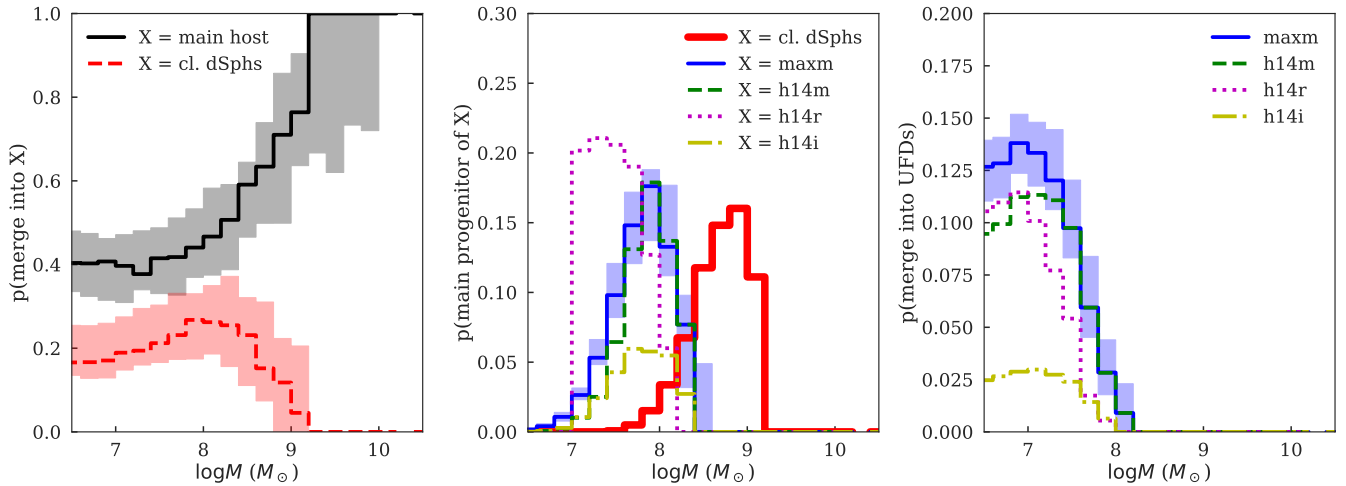


Figure 4. The fate of halos at $z = 8$ as a function of their mass at $z = 8$. Panel (a): At a given mass bin the fraction of $z = 8$ halos that merge into the main host and a classical dSph galaxy (defined by $M_{\star} > 2 \times 10^5 M_{\odot}$ using the abundance matching model of Garrison-Kimmel et al. 2014). Panel (b): shows the probability of becoming the main progenitor of a classical dSph galaxy (thick red line) and a surviving UFD at $z = 0$. Panel (c): The probability that a $z = 8$ halo has merged into a surviving UFD but is *not* the main progenitor of the UFD. For example, $\approx 40\%$ of $10^{7.5} M_{\odot}$ halos at $z = 8$ have merged into the main host, at the same mass bin $\approx 20\%$ merge into other classical dSph, $\approx 5 - 15\%$ survive as UFDs, and less than 10% merge into a UFD candidate at $z = 0$. In all panels, the lines indicate the median in each mass, shaded bars indicate 68% halo-to-halo scatter.

scale where being the main progenitor of the UFD peaks. For example at $z = 4$, halos with mass $\approx 10^{8.5} M_{\odot}$ have the highest chance of being the main progenitor of the UFD candidates and the probability distribution of the other progenitors drops to zero for masses above $\approx 10^{8.5} M_{\odot}$. Meanwhile, halos as small as $\approx 10^7 M_{\odot}$ have no chance of being the main progenitor of a UFD at $z = 4$, while they can be merge into the main progenitor of a UFD with probability of around 10%.

3.3 Informants other than mass

In this section we study whether knowledge of dynamical parameters of the halos other than their mass can be useful in predicting their survivability as UFD hosts today. Figure 6 shows the survivability in the 2D space for all the halos (in the top row) and for UFDs given the AM technique by which they are identified. Each row shows a different method to identify UFD candidates at $z = 0$ where the top row indicates the survival chance for all halos. We see a trend with lower virial ratio and larger distance from the main progenitor. Whether the concentration parameter affects the halo’s survival remains inconclusive. Note that the AM technique adopted in the **h14i** predicts less of a trend with virial ratio (lower probability at the same $(M, \log \eta)$ bin compared to the three other AM techniques. As we will discuss in Section 4, lower virial ratio is indicative of higher formation redshift or no recent merger activity and in the **h14i** model it is not the oldest that survives preferentially. The probability of survival of halos in the **h14i** model is on average about 1/3 of the other three AM techniques. At a given mass bin, one can select halos with low virial ratios or large distances from the main host to potentially boost the survival chance by a factor ≈ 3 .

Figure 7 shows the trends with redshift to see whether a

parameter becomes a stronger informant at higher or lower redshifts compared to the $z = 8$ results presented above. We show the results for two different methods of selecting UFDs at $z = 0$ (**maxm** in the top row and **h14i** in the bottom row). The left panel of Figure 7 shows the probability to survive as a UFD as a function of mass at different redshifts. At lower redshifts, the preferred mass range with the highest chance of survival increases to larger masses. For example, halos in the mass range $\log(M/M_{\odot}) = 7 - 7.5$ at $z = 12$ have the highest chance of survival while halos in the mass range $\log(M/M_{\odot}) = 8 - 8.5$ at $z = 4$ have the highest probability to survive as a UFD identified by the **maxm** method. The data suggests that for the **maxm** method of defining UFDs, halos with higher concentration preferably survive at higher redshifts and it switches to those with lower concentration going to lower redshifts. There is no trend with concentration parameter if for example the **h14i** method is applied to identify the UFD candidates at $z = 0$. There appears to be no redshift trend with virial ratio. Moreover, being at larger distances seems to increase the chance of survival more effectively at higher redshifts.

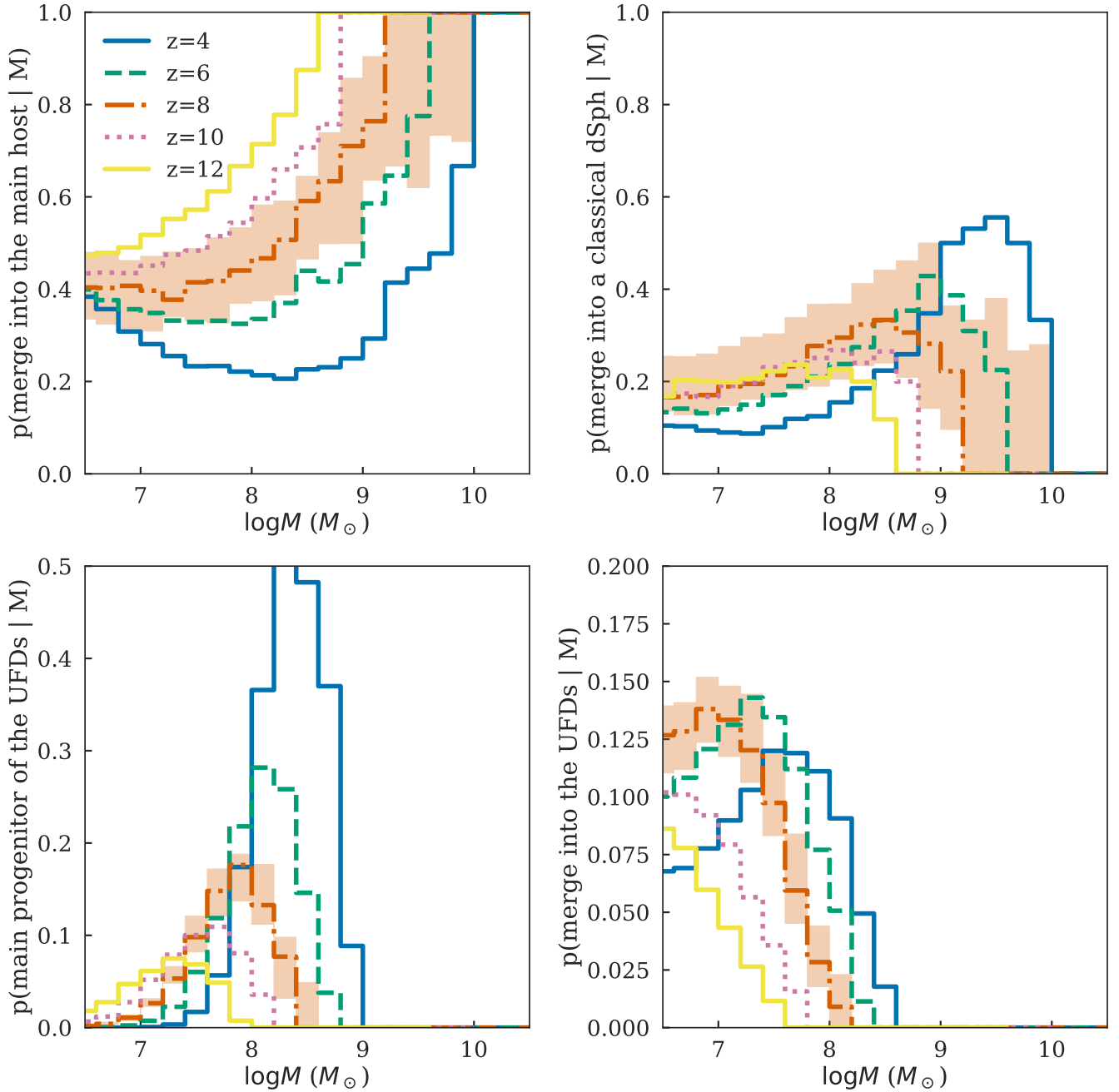


Figure 5. Same as Figure 4 but shown for different redshifts. Here we only use the “maxm” model to identify the UFD candidates. Panel (a): At a given mass, higher redshift halos have a higher probability to merge into the main host. For example a $10^8 M_\odot$ halo at $z = 12$ has a 60% chance of merging into the main host halo while the same mass halo at $z = 4$ has 20% chance to merge into the main host. The reason being the mass accretion of halos such that a $10^8 M_\odot$ halo at $z = 12$ would reach masses around $10^{10} M_\odot$ by $z = 4$. The general trend of more massive halos being more prone to merging is because of dynamical friction. See text for explaining the reason behind the upturn at low masses towards low redshifts. Panel (b): The probability of merging into a classical dSph galaxy becomes larger for more massive halos and at a given mass bin above $> 10^{8.5} M_\odot$ halos at lower redshifts have a higher probability to merge into a classical dSph galaxies while the situation reverses going to lower mass bins. Panel (c): The probability of being the main progenitor of a surviving UFD depends on mass and redshift of the halo. The peak of the probability shifts from lower masses at higher redshifts to higher masses at lower redshifts. Panel (d): The same trend is observed for halos merging into a surviving UFD.

4 SUMMARY AND DISCUSSION

The survival of subhalos has been extensively studied in the literature, and the results all suggest that the satellite-to-halo mass ratio and the orbit of the satellite are the key factors (Gnedin & Kravtsov 2006; Sales et al. 2007; Boylan-Kolchin et al. 2008; Penarrubia et al. 2008; Klimentowski et al. 2010; Bovill & Ricotti 2011; Garrison-Kimmel et al. 2017b). Yet, although the physical mechanism that determines the survival of the halos is well explored, the probability of surviving until $z = 0$ given a halo’s mass and other characteristics at higher redshifts is poorly studied. Gnedin & Kravtsov (2006) show that 5%-15% of subhalos in the mass range corresponding to dSph satellites at $z \approx 8$ survive until the present in a MW-like environment.

In this work, we extend these studies to the realm of UFDs. Our results are based on analysis of merger trees constructed from the *Caterpillar* simulation suite (Griffen et al. 2016b,a) which, consists of 32 MW type halos simulated with a mass resolution of $m_p \approx 10^4 M_\odot$, suitable to study UFD progenitors. We identified UFD candidates at $z = 0$ based on four selection criteria discussed in Hargis et al. (2014); Garrison-Kimmel et al. (2014), and trace all the halos in the zoom-in simulation box that will end up within the virial radius of a given MW type halo from high redshifts down to $z = 0$.

We find that a large fraction of the progenitor halos merge into dSph like subhalos or into the main host due to dynamical friction, but about 10% of the halos at $z = 8$ with $\log M/M_\odot = 7 - 8$ survive to the present day as UFD host candidates. At a given halo mass, the probability of survival decreases towards higher redshifts, because those halos represent more massive halos at lower redshifts, and are therefore they are more likely to merge into large subhalos or into the main host. We also consider the effect of three other parameters on UFD survival probability: concentration, virial ratio and distance from the main progenitor. Our results suggest that choosing halos with lower values of the virial ratio, which is indicative of higher formation redshift and a lack of recent merger activity (Power et al. 2012; Cui et al. 2017) or selecting halos at large comoving distances from the main progenitor ($D > 300\text{kpc}/h$), which is indicative of longer infall time, can boost the survival probability by a factor of ≈ 3 . The behavior with concentration parameter remains inconclusive, but the results suggest slightly higher chances of survival for halos with higher concentration if selected at higher redshifts, and lower concentration if selected at lower redshifts.

Three main uncertainties remain that could affect our N-body results. The first is the presence of baryons, which have the potential to have significant effects on the underlying dark matter distribution. This has been explored in other studies (Geen et al. 2013; Despali & Vegetti 2017; Sawala et al. 2017; Garrison-Kimmel et al. 2017b; Errani et al. 2017). For example, Sawala et al. (2017) explored the impact of including baryons on the statistics and spatial distribution of the satellites of a MW type halo in the mass range of $10^{6.5} - 10^{8.5} M_\odot$. They find the number of the satellites would be reduced by 25-50% independent of the satellite mass but that this effect would be increased toward the halo center. Similar results are presented in Garrison-Kimmel et al. (2017b) where by analyzing the Latte simu-

lation suite (Wetzel et al. 2016), demonstrate the presence of the galactic disk as the main reason why baryons impact the statistics of the small satellites compared to DM-only simulations.

A second uncertainty is the limit of the minimum subhalo mass that is able to host a MW satellite galaxy (Dooley et al. 2016a; Jethwa et al. 2016). Halos below the atomic cooling limit, which corresponds to a mass $\approx 10^8 M_\odot$ during reionization, cool via H_2 and fine structure line cooling and their stellar mass content is sensitive to the effect of feedback from their first generation of stars. The Far Ultraviolet (FUV) radiation from the first generation of stars can destroy the H_2 , which is the primary coolant (negative feedback; Machacek et al. 2001; O’Shea & Norman 2008), or help the cooling efficiency through the formation of H^- (positive feedback; Haiman et al. 1996). Such considerations can theoretically constrain the lower limit on the host halo mass of UFDs that could survive until present day. However, below $M_h < 10^8 M_\odot$, star formation becomes a stochastic process that increases the scatter in the $M_\star - M_h$ relationship and leads to different behavior for halos below the atomic cooling limit (Chen et al. 2014; Garrison-Kimmel et al. 2017a). For example, studying individual halos through a set of hydrodynamical simulations, Bland-Hawthorn et al. (2015) showed that the lowest possible mass of a UFD progenitor is $\approx 10^7 M_\odot$, as halos below this mass cannot survive the energy input of a single SN explosion, despite the presence of radiative cooling. On the other hand, by performing zoom-in hydrodynamical simulations on galaxies and UFDs, Wheeler et al. (2015b) concluded that $M_h \approx 5 \times 10^9 M_\odot$ is minimum halo mass threshold, while Jeon et al. (2017) performed cosmological simulations of individual LG galaxies within the LG to show that $M_h \approx 10^9 M_\odot$ form 90% of their stars prior to the reionization.

Finally, better constraints on UFD progenitor halo could be determined if the $z = 0$ properties of UFD halos were better known. Though UFDs are likely ubiquitous in the universe (e.g. Lee et al. 2017), their low luminosities make them currently observable only as Milky Way satellites. Even at these distances, poorly estimated incompleteness limits our determination of their luminosity function and radial distribution (e.g. Koposov et al. 2008; Newton et al. 2017). Their color magnitude diagrams and chemical abundance distributions of UFDs clearly point to systems that formed all their stars within the first two Gyr of the universe (Vargas et al. 2013; Brown et al. 2014; Weisz et al. 2014; Frebel et al. 2014), but the masses, concentrations, and virial parameters of dark matter halos they contain are poorly constrained due to the relatively small number of stars currently accessible with spectroscopy. Thus, direct constraints on UFD dynamical masses are restricted to the stellar half light radius (Wolf et al. 2010), and inferring the total halo mass of a UFD requires extrapolating an assumed density profile beyond the stellar observations (e.g. Strigari et al. 2008).

Despite these issues, our results can be used as a rough guide to those performing zoom-in simulations on UFD candidates (e.g. Safarzadeh & Scannapieco 2017; Jeon et al. 2017), as they allow for analyses of a limited sample of halos at high redshifts without the need to trace the simulations down to $z = 0$. Given the survival statistics presented in this paper, one can carefully select high-redshift halos, based on

their mass and other characteristics, and study them in detail knowing the probability of them to survive as UFD candidates at $z = 0$. [Boylan-Kolchin et al. \(2016\)](#) have shown that the LG progenitors at redshifts $z > 8$ have a linear comoving size of ≈ 8 Mpc/h and are large enough to be cosmologically representative in terms of matter density and counts of dark matter halos with $M_{\text{vir}}(z = 7) < 2 \times 10^9 M_{\odot}$. Therefore, if one simulates a cosmological volume of similar size down to the reionization redshift, that volume could end up hosting a LG at $z = 0$.

Adopting the survival statistics of the halos that we present above would imply that, out of N halos selected from such simulations at a given mass bin and redshift with survival probability of $P_s(M, z)$, the chances that at least one of them become a UFD host candidate at $z = 0$ is $P = 1 - (1 - P_s(M, z))^N$. Therefore if we select 20(10) halos with survival chance of 10(20)%, there is $\approx 90\%$ chance that at least one of them will end up as a UFD host candidate at $z = 0$. Considering other characteristics that boost the survival as UFD candidates by a factor of ≈ 3 would lead to only a handful of halos needed to be simulated at high redshifts to confidently generate at least one $z = 0$ UFD host candidate. Future work on this topic, including baryonic effects and studying other halo properties, may be able to improve these probabilities further, boosting the reliability of near field cosmological studies by better selecting ultra-faint dwarf candidate progenitors in high redshifts cosmological simulations.

5 ACKNOWLEDGEMENTS

We are thankful to Mia Bovill, Brendan Griffen, John Wise and Daniel Weisz for useful discussions. MTS is supported by the National Science Foundation under grant AST14-07835 and by NASA under theory grant NNX15AK82G. APJ is supported by NASA through Hubble Fellowship grant HST-HF2-51393.001 awarded by the Space Telescope Science Institute, which is operated by the Association of Universities for Research in Astronomy, Inc., for NASA, under contract NAS5-26555. This research is supported in part by the National Science Foundation (NSF; USA) under grant No. PHY-1430152 (JINA Center for the Evolution of the Elements). B.W.O. was supported by the National Aeronautics and Space Administration (NASA) through grant NNX15AP39G and Hubble Theory Grant HST-AR-13261.01-A, and by the NSF through grant AST-1514700. Computational support for the Caterpillar simulations were provided by XSEDE through the grants (TG-AST120022, TG-AST110038). We further acknowledge support of the computer cluster of the MIT Astrophysics Division, which was built with support from the Kavli Investment Fund administered by the MIT Kavli Institute for Astrophysics and Space Research.

REFERENCES

- Behroozi P. S., Wechsler R. H., Wu H.-Y., 2013a, *ApJ*, **762**, 109
 Behroozi P. S., Wechsler R. H., Wu H.-Y., 2013b, *The Astrophysical Journal*, **762**, 109
 Behroozi P. S., Wechsler R. H., Wu H.-Y., Busha M. T., Klypin A. A., Primack J. R., 2013c, *ApJ*, **763**, 18
 Behroozi P. S., Wechsler R. H., Conroy C., 2013d, *The Astrophysical Journal*, **770**, 57
 Bland-Hawthorn J., Sutherland R., Webster D., 2015, *The Astrophysical Journal*, **807**, 154
 Bovill M. S., Ricotti M., 2009, *The Astrophysical Journal*, **693**, 1859
 Bovill M. S., Ricotti M., 2011, *The Astrophysical Journal*, **741**, 17
 Boylan-Kolchin M., Ma C.-P., Quataert E., 2008, *Monthly Notices of the Royal Astronomical Society*, **383**, 93
 Boylan-Kolchin M., Weisz D. R., Bullock J. S., Cooper M. C., 2016, *Monthly Notices of the Royal Astronomical Society: Letters*, **462**, L51
 Brook C. B., Di Cintio A., Knebe A., Gottlöber S., Hoffman Y., Yepes G., Garrison-Kimmel S., 2014, *The Astrophysical Journal*, **784**, L14
 Brown T. M., et al., 2014, *The Astrophysical Journal*, **796**, 91
 Bryan G. L., Norman M. L., 1998, *ApJ*, **495**, 80
 Bullock J. S., Kravtsov A. V., Weinberg D. H., 2000, *The Astrophysical Journal*, **539**, 517
 Chandrasekhar S., 1943, *The Astrophysical Journal*, **97**, 255
 Chen P., Wise J. H., Norman M. L., Xu H., O’Shea B. W., 2014, *The Astrophysical Journal*, **795**, 144
 Cui W., Power C., Borgani S., Knebe A., Lewis G. F., Murante G., Poole G. B., 2017, *Monthly Notices of the Royal Astronomical Society*, **464**, 2502
 Despali G., Vegetti S., 2017, *Monthly Notices of the Royal Astronomical Society*, **469**, 1997
 Dooley G. A., Griffen B. F., Zuckin P., Ji A. P., Vogelsberger M., Hernquist L. E., Frebel A., 2014, *The Astrophysical Journal*, **786**, 50
 Dooley G. A., Peter A. H. G., Yang T., Willman B., Griffen B. F., Frebel A., 2016a, eprint arXiv:1610.00708
 Dooley G. A., Peter A. H. G., Yang T., Willman B., Griffen B. F., Frebel A., 2016b, preprint, ([arXiv:1610.00708](#))
 Drlica-Wagner A., et al., 2015, *The Astrophysical Journal*, **813**, 109
 Errani R., Penarrubia J., Laporte C. F. P., Gómez F. A., 2017, *Monthly Notices of the Royal Astronomical Society: Letters*, **465**, L59
 Fattahi A., et al., 2016, *Monthly Notices of the Royal Astronomical Society*, **457**, 844
 Frebel A., Bromm V., 2012, *The Astrophysical Journal*, **759**, 115
 Frebel A., Simon J. D., Kirby E. N., 2014, *The Astrophysical Journal*, **786**, 74
 Garrison-Kimmel S., Boylan-Kolchin M., Bullock J. S., Lee K., 2014, *Monthly Notices of the Royal Astronomical Society*, **438**, 2578
 Garrison-Kimmel S., Bullock J. S., Boylan-Kolchin M., Bardwell E., 2017a, *Monthly Notices of the Royal Astronomical Society*, **464**, 3108
 Garrison-Kimmel S., et al., 2017b, *Monthly Notices of the Royal Astronomical Society*, **471**, 1709
 Geen S., Slyz A., Devriendt J., 2013, *Monthly Notices of the Royal Astronomical Society*, **429**, 633
 Gnedin N. Y., Kravtsov A. V., 2006, *The Astrophysical Journal*, **645**, 1054
 Griffen B. F., Dooley G. A., Ji A. P., O’Shea B. W., Gómez F. A., Frebel A., 2016a, arXiv.org, p. arXiv:1611.00759
 Griffen B. F., Ji A. P., Dooley G. A., Gómez F. A., Vogelsberger M., O’Shea B. W., Frebel A., 2016b, *The Astrophysical Journal*, **818**, 10
 Hahn O., Abel T., 2011, *MNRAS*, **415**, 2101
 Haiman Z., Rees M. J., Loeb A., 1996, *The Astrophysical Journal*, **467**, 522
 Hargis J. R., Willman B., Peter A. H. G., 2014, *The Astrophysical Journal*, **795**, L13
 Jeon M., Besla G., Bromm V., 2017

- Jethwa P., Belokurov V., Erkal D., 2016, eprint arXiv:1612.07834
- Kirby E. N., Simon J. D., Geha M., Guhathakurta P., Frebel A., 2008, *The Astrophysical Journal*, 685, L43
- Klimentowski J., Lokas E. L., Knebe A., Gottlöber S., Martínez-Vaquero L. A., Yepes G., Hoffman Y., 2010, *Monthly Notices of the Royal Astronomical Society*, 402, 1899
- Koposov S., et al., 2008, *The Astrophysical Journal*, 686, 279
- Koposov S. E., Belokurov V., Torrealba G., Evans N. W., 2015, *The Astrophysical Journal*, 805, 130
- Kravtsov A. V., Gnedin O. Y., Klypin A. A., 2004, *The Astrophysical Journal*, 609, 482
- Lee M. G., Jang I. S., Beaton R., Seibert M., Bono G., Madore B., 2017, *The Astrophysical Journal Letters*, 835, L27
- Lu Y., Benson A., Wetzel A., Mao Y.-Y., Tonnesen S., Peter A. H. G., Boylan-Kolchin M., Wechsler R. H., 2017, *The Astrophysical Journal*, 846, 66
- Machacek M. E., Bryan G. L., Abel T., 2001, *The Astrophysical Journal*, 548, 509
- McConnachie A. W., 2012, *The Astronomical Journal*, 144, 4
- Moster B. P., Naab T., White S. D. M., 2013, *Monthly Notices of the Royal Astronomical Society*, 428, 3121
- Newton O., Cautun M., Jenkins A., Frenk C. S., Helly J., 2017, eprint arXiv:1708.04247
- O’Shea B. W., Norman M. L., 2008, *The Astrophysical Journal*, 673, 14
- Penarrubia J., Navarro J. F., McConnachie A. W., Martin N. F., 2008, arXiv.org, pp 222–232
- Planck Collaboration et al., 2014, *A&A*, 571, A16
- Power C., Knebe A., Knollmann S. R., 2012, *Monthly Notices of the Royal Astronomical Society*, 419, 1576
- Safarzadeh M., Scannapieco E., 2017, *Monthly Notices of the Royal Astronomical Society*, 471, 2088
- Sales L. V., Navarro J. F., Abadi M. G., Steinmetz M., 2007, *Monthly Notices of the Royal Astronomical Society*, 379, 1464
- Salvadori S., Ferrara A., 2009, *Monthly Notices of the Royal Astronomical Society*, 395, L6
- Sawala T., Pihajoki P., Johansson P. H., Frenk C. S., Navarro J. F., Oman K. A., White S. D. M., 2017, *Monthly Notices of the Royal Astronomical Society*, 467, 4383
- Simon J. D., Geha M., 2007, *The Astrophysical Journal*, 670, 313
- Simon J. D., et al., 2011, *The Astrophysical Journal*, 733, 46
- Springel V., 2005, *MNRAS*, 364, 1105
- Springel V., et al., 2008, *Monthly Notices of the Royal Astronomical Society*, 391, 1685
- Strigari L. E., Koushiappas S. M., Bullock J. S., Kaplinghat M., Simon J. D., Geha M., Willman B., 2008, *The Astrophysical Journal*, 678, 614
- Tollerud E. J., Bullock J. S., Strigari L. E., Willman B., 2008, *The Astrophysical Journal*, 688, 277
- Vargas L. C., Geha M., Kirby E. N., Simon J. D., 2013, *The Astrophysical Journal*, 767, 134
- Weisz D. R., Dolphin A. E., Skillman E. D., Holtzman J., Gilbert K. M., Dalcanton J. J., Williams B. F., 2014, *The Astrophysical Journal*, 789, 148
- Wetzel A. R., Hopkins P. F., Kim J.-h., Faucher-Giguère C.-A., Kereš D., Quataert E., 2016, *The Astrophysical Journal Letters*, 827, L23
- Wheeler C., Oñorbe J., Bullock J. S., Boylan-Kolchin M., Elbert O. D., Garrison-Kimmel S., Hopkins P. F., Kereš D., 2015a, *MNRAS*, 453, 1305
- Wheeler C., Oñorbe J., Bullock J. S., Boylan-Kolchin M., Elbert O. D., Garrison-Kimmel S., Hopkins P. F., Kereš D., 2015b, *Monthly Notices of the Royal Astronomical Society*, 453, 1305
- Wolf J., Martínez G. D., Bullock J. S., Kaplinghat M., Geha M., Muñoz R. R., Simon J. D., Avedo F. F., 2010, *Monthly Notices of the Royal Astronomical Society*, 406, 1220
- Xu H., Wise J. H., Norman M. L., Ahn K., O’Shea B. W., 2016, *The Astrophysical Journal*, 833, 84

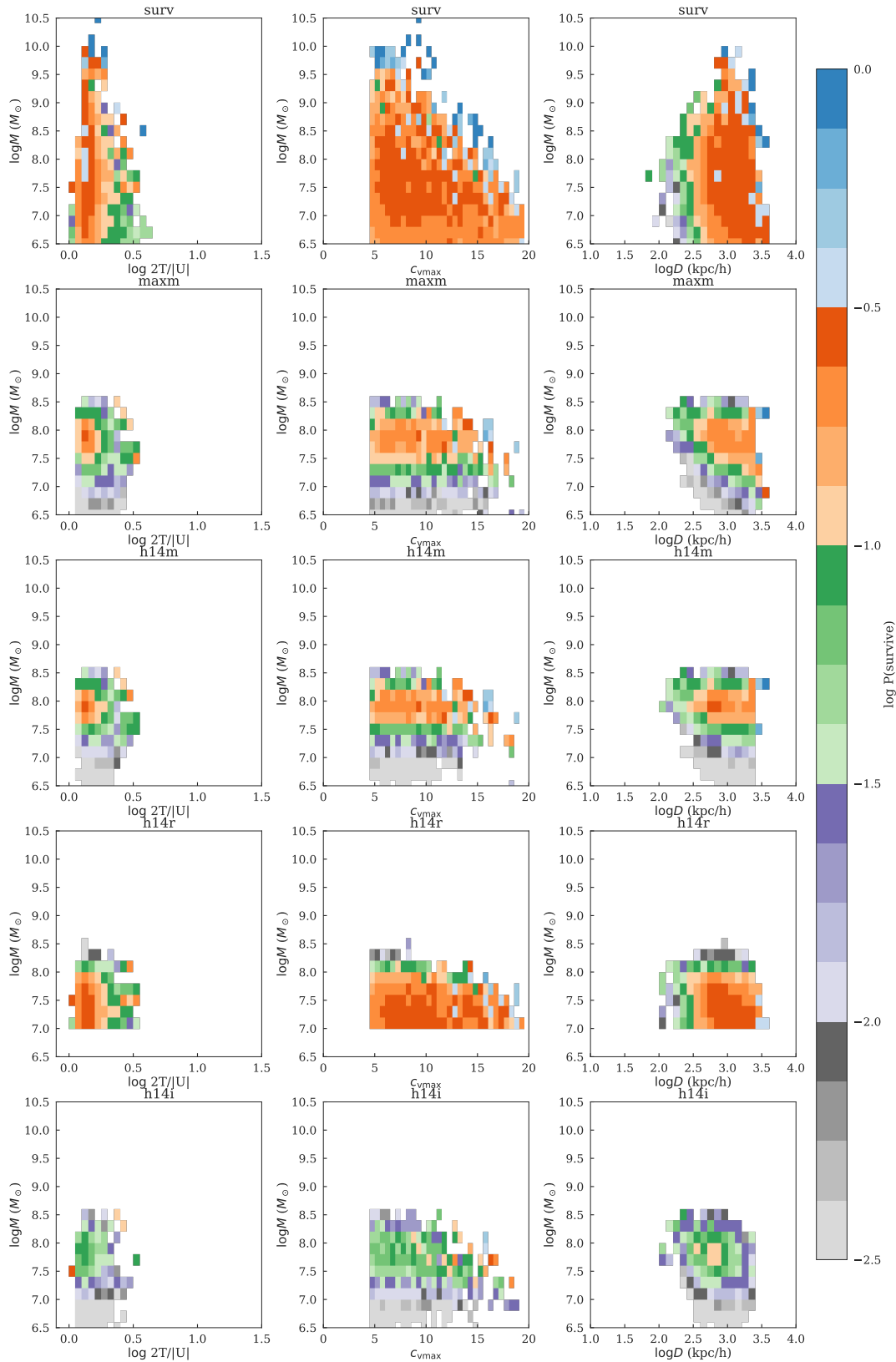


Figure 6. The survival probability of all the halos as UFDs in the 2D space of mass *and* virial ratio (first column), concentration (second column) and distance from the main progenitor (third column) at $z = 8$. The color coding is showing the probability of survival. Each row corresponds to a different AM technique to select satellite UFD candidates at $z = 0$. At a given mass bin, selecting halos with lower virial ratio and with larger distance from the main progenitor boosts their chance of survival as UFDs by a factor of ≈ 3 . The trend with concentration parameter remains inconclusive.

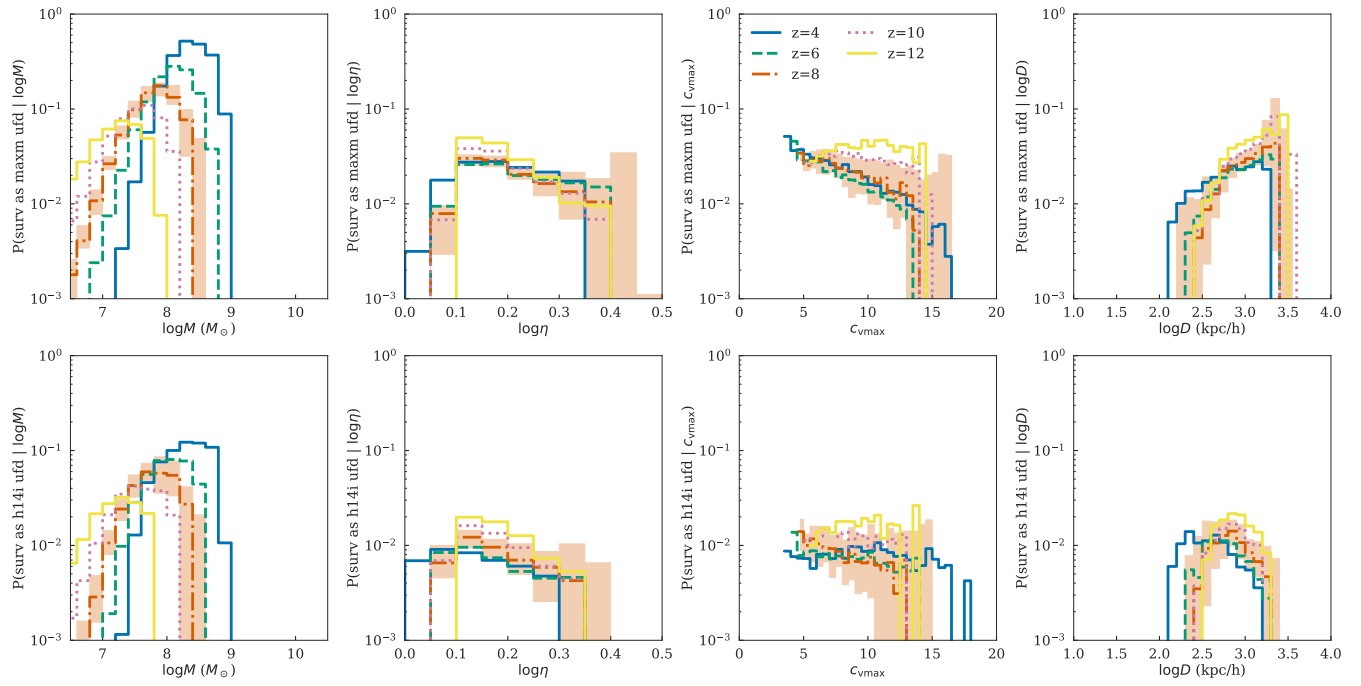


Figure 7. The trend of survival probability as a UFD at a given redshift for different dynamical parameters. Top row: **maxm** method is adopted to define a UFD at $z = 0$. The data suggests that the halos with higher concentration preferably survive at higher redshifts and it switches to those with lower concentration as we go to lower redshifts. The trend with mass is discussed before and the trend with other parameters remain less dependent on the redshift of consideration. Bottom row: **h14i** method is adopted to define a UFD at $z = 0$. The same trends as in the top row are observed, however, the concentration is flatter at all redshifts. In other words, the **h14i** method shows no preference in selecting halos if it is only based on the concentration parameter.